Threshold dynamics of $L_{2,3}M_{4,5}M_{4,5}$ Auger satellites in $4d$ metals

W. Drube, T. M. Grehk,* R. Treusch, and G. Materlik
Hamburger Synchrotronstrahlungslabor HASYLAB am Deutschen Elektronen-Synchrotron DESY, Notkestrasse 85, D-22603 Hamburg, Germany

J. E. Hansen
Department of Physics and Astronomy, University of Amsterdam, Valckenierstraat 65, NL-1018XE Amsterdam, The Netherlands

T. Åberg
Laboratory of Physics, Helsinki University of Technology, P.O. Box 1100, FIN-02015 HUT, Finland
(Received 15 June 1999)

The near $L_{2,3}$-threshold photon energy dependence of the satellite structures in $4d$ metals has been studied. In Ru and Rh there is one satellite. It exhibits the same threshold resonance behavior as the main lines identifying its origin as a final-state screening effect. Two different types are observed for Pd: one like in Ru and Rh and another one that disperses relative to the main line up to about 7 eV above threshold. Then its position is fixed, and its absolute intensity shows a modulation opposite to that of the main line. We attribute this satellite to a final-state shake mechanism and find a related feature also in Ag, which, however, has a monotonic intensity development. [S0163-1829(99)01647-1]

Resonant Auger spectra of atoms and molecules have very recently revealed unexpected dynamics of core hole formation.[1–4] Features appear that cannot be directly related to the diagram lines. Some of these structures appear close to an inner-shell threshold as distinct satellites. In solids, collective excitations may also give rise to satellites both through intrinsic and extrinsic processes.[5] The interpretation of satellites, however, is generally not straightforward for solids.[6–9] In particular, if the nature of the underlying mechanism is atomiclike, their origin is often controversial. Solid d-band materials are especially intriguing because the valence shell generally comprises both delocalized and localized levels. The subtle interplay between solid state (band) and atomic behavior is related to the degree of d-band filling, i.e., closed shell vs open shell character. This is very relevant for the satellite structure in the Auger spectra of these materials. The $L_{2,3}M_{4,5}M_{4,5}$ transitions of the solid 3d metals have been studied for many years from this point of view. Pronounced satellites are observed for Ni, Cu, and Zn,[6,10–12] whereas Co and Fe show negligible satellite contributions.[13] The situation is, however, complicated since the final-state holes are in the valence band, and therefore, the corresponding states mix with the band states.[14–16]

Much less work is reported on the corresponding purely inner-shell transition in the $4d$ metals. Nevertheless, in the available data[8,17–20] a satellite structure is observed not only for Pd and Ag, but also—in contrast to Fe and Co—for Ru and Rh. For the $3d$ metals a spectator-type transition in the presence of a $3d$ vacancy is proposed to account for the satellites, but this is debated.[6,7,14] Even using synchrotron radiation, the interpretation of the $L_{2,3}M_{4,5}M_{4,5}$ satellites in the $3d$ metals is difficult not only because the final holes reside in the valence shell but also because the initial $L_{2,3}$ splitting is comparable to the energy span of the entire spectra. More seriously, the near $L_{2,3}$ threshold spectra strongly overlap the valence photoemission spectrum. For the $4d$ metals, on the other hand, the situation is quite different and much clearer because the entire $L_{2,3}M_{4,5}M_{4,5}$ transition takes place between inner-shell states. The purely atomic character is supported by an atomic Hartree-Fock calculation in intermediate coupling including the spin-orbit interaction.[21] Indicated in Fig. 1 is the result for the Auger spectrum between the $2p^5 3d^{10} 4d^{10}$ initial and $2p^6 3d^8 4d^{10}$ final states in Ag, which is in good agreement with the measured distribution of

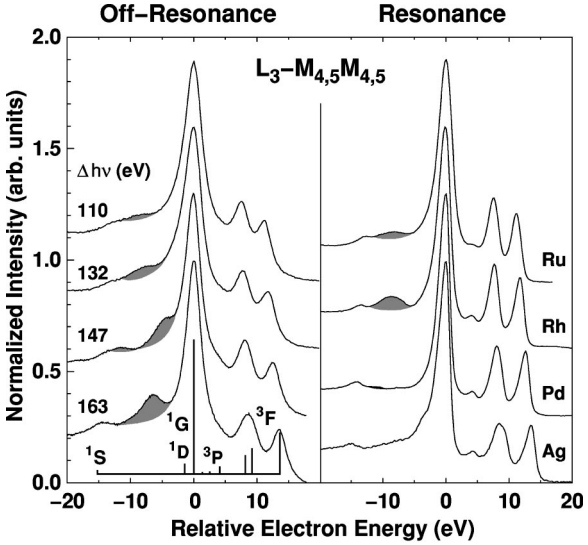

FIG. 1. L_3-$M_{4,5}M_{4,5}$ spectra for the studied $4d$ metals excited far above (left) and close to (right) the L_3 threshold. The figure shows raw data; a constant background has been subtracted. The electron energies are aligned relative to the prominent ^1G line; peak maxima are normalized to unity. The ^1G kinetic energy ranges from 2250 eV (Ru) to 2577 eV (Ag). Note the significant line narrowing for resonant excitation and the markedly different behavior of the satellite structures below the main line. A calculation for atomic Ag is shown for comparison.

diagram lines. The decay rates are calculated using perturbation theory taking continuum p and f waves into account separately. The energies are aligned relative to ^1G.

The origin of the extra satellite structure is not obvious from the conventionally excited spectra[17–20] alone. In the present experiment, high intensity monochromatic synchrotron x-rays are used to selectively fine tune the excitation through the $L_{2,3}$ thresholds[22] and monitor the evolution of the satellite structures. The data obtained on the resonantly excited $L_{2,3}M_{4,5}M_{4,5}$ transitions reveal unprecedented detail of the dynamical satellite behavior. In particular, it is observed that the satellite emission below the main ^1G Auger line shows a dramatically different resonance behavior for Ru and Rh compared to Pd and Ag, which is direct evidence for distinctly different mechanisms.

High-resolution resonant photoemission studies for these inner-shell L_2 and L_3 levels became possible only recently through the combination of intense synchrotron radiation x-rays with state-of-the-art electron detection techniques.[23] The data were obtained with the tunable high-energy x-ray photoelectron spectroscopy instrument at the wiggler beamline BW2 of HASYLAB. The photon flux from the Si(111) double crystal monochromator typically amounts to $3 \times 10^{12} s^{-1}$ on the sample. At a photon energy $h\nu = 3000$ eV, the spectral bandpass is 0.5 eV. The electrons were measured using a hemispherical analyzer with parallel detection capability (SCIENTA SES-200); the resolution was set to 0.2 eV. High-purity metal foils, cleaned in ultrahigh vacuum, were used as samples. For the threshold studies, $h\nu$ is measured relative to the $L_{2,3}$ absorption edges as obtained from total electron yield data. The relative energy $\Delta h\nu$ is accurate to ± 0.1 eV, which was achieved by frequently referencing suitable photoelectron lines. All electron spectra were normalized to the photon flux.

In order to understand the evolution of the spectra as a function of $h\nu$, one must consider the overall behavior of the threshold Auger process, which can be viewed as nonradiative inelastic scattering occurring as a single quantum-mechanical event.[24,25] In the experiment, the gradual transition from nonradiative resonant Raman-like scattering to characteristic Auger electron emission is revealed as $h\nu$ is tuned through the threshold.

A fingerprint for the resonant one-step nature of the process is a characteristic sub-lifetime line narrowing that is observed if the combined spectral and analyzer bandwidths are smaller than the intermediate hole lifetime. Another fingerprint is an energy dispersion of various scattering features proportional to $h\nu$. It has also been demonstrated experimentally that even for deep inner-shell transitions the valence shell comes into play through the intermediate excited hole states by way of the symmetry-projected density of unoccupied states.[8] Here, all these known characteristics of the main lines are taken into account in the evaluation of the satellite behavior across threshold.

The different nature of the satellites becomes apparent if off-resonance excited spectra are compared to the corresponding resonance data (Fig. 1). The satellite emission observed below the prominent ^1G Auger line is indicated as shadowed areas. The left panel displays the $L_3M_{4,5}M_{4,5}$ energy distribution curves obtained for high excess energies $\Delta h\nu$ above the L_3 edge but still well below L_2 ($< L_2 - 10$ eV). This rules out a spectator-hole mechanism due to L_2L_3N Coster-Kronig transitions as an origin of any of the satellites. The spectra change dramatically for resonant excitation (right panel): the satellites for both Ag and Pd are strongly suppressed whereas for Rh and Ru they remain and become even more pronounced. This goes along with the overall resonant sublifetime line narrowing observed for the main lines. Note that in the resonantly excited Ag spectrum a marked shoulder is observed on the low-energy side of the ^1G line. This feature is inherent to the Ag threshold Auger process, and it is caused, as just mentioned, by density-of-state modulations in the intermediate excited state.[8]

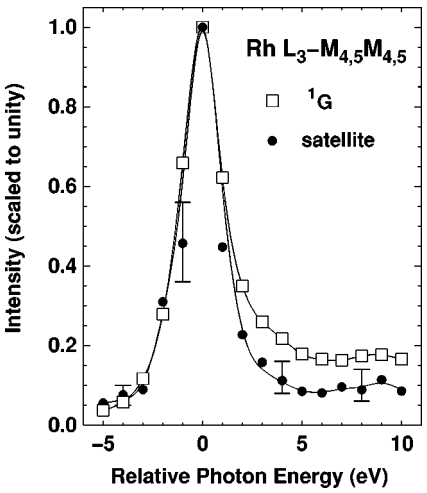

FIG. 2. Threshold resonance behavior of the Rh -8.6 eV satellite intensity (circles) compared to the ^1G line (squares). The photon energy is measured relative to the peak of the L_3 absorption.

We now focus on the detailed $h\nu$ dependence of the satellite emission below the ^1G lines. In Fig. 2 the near threshold Rh satellite intensity is compared to that of ^1G. Because the Auger line shapes continuously modulate throughout the studied $h\nu$ range ($\Delta h\nu \approx +45$ eV), we have approximated the low-energy tail of the ^1G line by a Lorentzian in each spectrum separately, which was then subtracted from the raw data to extract the satellite peak. The satellite intensity was obtained by integrating the peak in the difference spectrum within a 5-eV interval. We note that the satellite has a fixed energy (-8.6 ± 0.1 eV) relative to ^1G. It is obvious from the data that the satellite intensity mimics the behavior of the main line. The resonance develops a strong intensity maximum, a ''white line,'' at the $L_{2,3}$ absorption edge, which is due to intermediate states with a $2p$ electron excited into localized unoccupied $4d$ states. A resonance line narrowing at threshold, which is characteristic of the behavior of the main lines, is also observed for the satellite peak.

Although less intense, the Ru satellite behaves in the same way. Since the Ru and Rh satellites exhibit a threshold behavior similar to ^1G, they must have a common origin related to that line. We therefore associate them with different final-state configurations but the same intermediate state. According to the pure atomic picture, Ru and Rh would have a final-state multiplet structure that corresponds to $3d^8 4d^7 5s$ and $3d^8 4d^8 5s$, respectively. In the solid, it is reasonable to introduce an additional $4d$-type screening orbital in the final state, and the corresponding configurations would read $3d^8 4d^{x+1}$ ($x = 7,8$). The satellite can then be due to final

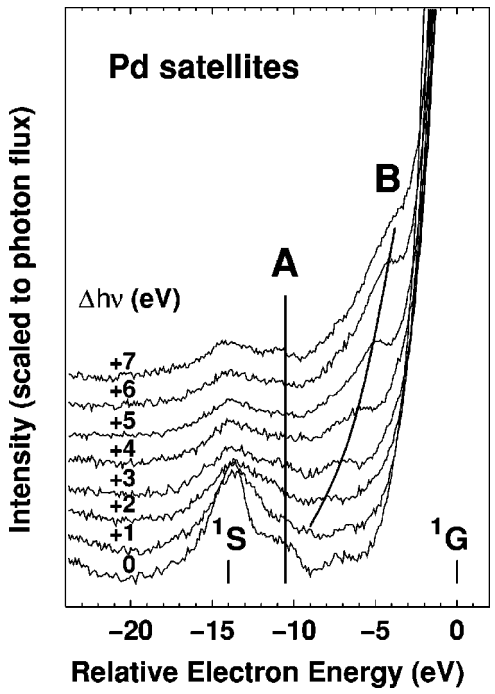

FIG. 3. Close-up of the Pd satellite region for near threshold excitation. $\Delta h\nu = 0$ eV refers to the peak of the L_3 absorption edge. Satellite *A* stays at constant relative energy; *B* disperses up to $\Delta h\nu \approx +7$ eV while gaining intensity.

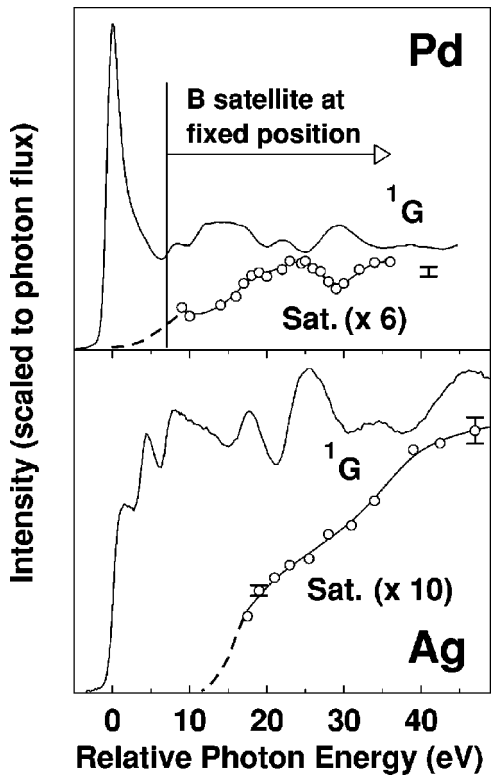

FIG. 4. Intensity development of the Pd and Ag ^1G lines and their satellites above threshold. The dashed lines qualitatively show the onset of the satellite intensity.

states associated with $3d^8 4d^x 5s$ located closeby, when 5s is a localized orbital in the presence of two $3d$ holes.

From the atomic Hartree-Fock calculation for Rh, the total energy differences (mean values) between the final $2p^6 3d^8 4d^8 5s$ and $2p^6 3d^8 4d^9$ states are obtained. It is found that the energy of the Auger transition for the $3d^8 4d^8 5s$ configuration is lower by 10 eV.

The observed spectrum can therefore be understood by assuming that the main spectrum, i.e., the $3d^8 4d^9$ final-state multiplet, is accompanied by a low-energy replica and that the observed satellite is due to the strongest line (^1G). It is noted that both the $3d^8 4d^x 5s$ and the $3d^8 4d^{x+1}$ spectra are somewhat broadened by multiplet splitting due to coupling of the two open *d* subshells. Their calculated energy separation, 10 eV (see above), is in accordance with the observed relative satellite position shown in Fig. 1. As further evidence for this final-state effect, we find the same resonance behavior (cf. Fig. 2) for the L_2 spectra.

In Pd and Ag, the situation is different because the $4d$ subshell is almost or completely filled. Accordingly, the screening features should be suppressed or absent. Indeed, for the resonance case shown in Fig. 1, no satellite is observed for Ag, because the completely filled $4d$ subshell excludes $4d$ screening.

For large $\Delta h\nu$, however, both metals also develop distinct satellites. For Pd, two broad features are observed at -11.3 ± 0.1 eV and -4.8 ± 0.1 eV, respectively. Closer inspection of the Pd threshold spectra (Fig. 3) shows that these satellites, labeled *A* and *B*, are still present although weak. We now focus on their behavior as the excitation energy is raised above threshold. Since in the Raman-like regime below threshold the *absolute* kinetic energy of the *entire* final-state structure depends linearly on $h\nu$, we prefer to align the energies relative to ^1G in order to avoid confusion. It is found that the two Pd satellites exhibit a completely different dynamic behavior. Structure *A* has a constant energy relative to ^1G while *B* disperses roughly linearly *relative* to this line up to $\Delta h\nu \approx +7$ eV and at the same time is gaining intensity. Feature *B* appears to merge into A at $\Delta h\nu \approx 0$ eV. There is no further relative change for subthreshold excitation energies. The small additional feature near -7 eV in the lowest spectrum is interpreted as a modulation induced by structure in the unoccupied density of *d* states (as described above for Ag).

Since the *A* satellite is rather weak and partly overlaps with the ^1S diagram line, it is difficult to extract an $h\nu$ dependence of its intensity. Its relative position, however, is fixed, and it is thus of similar nature as the satellites in Ru and Rh. Hence, we attribute it to partial $4d$ screening in the final state.

In the following, the Pd (*B*) and Ag satellites are discussed. These features are not explained by the model described above; instead we ascribe their origin to a final-state shake mechanism as outlined below. The satellite evolution for larger excess excitation energies is shown in Fig. 4. It is now well established that the intensities and the line shapes of the Auger diagram lines continuously modulate up to quite high excess energies in solids.[8] Therefore, it is not meaningful to discuss the satellite structures in terms of relative intensities. Instead, we compare the intensity modulation of both ^1G and the satellites on an *absolute* scale. While the modulation of the main lines mimics the L_3 absorption spectrum, the satellites exhibit a totally different behavior. Above $\Delta h\nu \approx +7$ eV, where the position of the Pd *B* satellite rela-

tive to ^1G is fixed, its intensity modulation appears to be opposite to that of ^1G. In Ag, the satellite emerges at constant relative energy and exhibits a monotonic increase without any obvious fine structure.

The $h\nu$ dependence of the Pd B satellite *position*, dispersive vs fixed, can be understood by implementing an extra (shake) excitation in the final state. Since the $4d$ shell is almost filled in Pd, the excited final-state configuration would be $3d^8 4d^9 \epsilon' d$. If $\epsilon' d$ is quasibound, then there is linear dispersion of the corresponding satellite with respect to ^1G. Note, that this behavior is analogous to the dispersion of the main Auger lines in the subthreshold regime. An excitation to such a state can only occur from intermediate states with local $4d$ character, i.e., in the region of the sharp peak shown in Fig. 4. The nondispersive part at higher excitation energies then relates to intermediate states that are less local. The change from dispersive to nondispersive behavior thus marks a transition from shake up to shake off.

Since there are no local empty $4d$ states in Ag, there is no shake-up but only a shake-off satellite with a delayed onset. The different intensity behavior in Pd and Ag pertains to the nature of the screening of the two $3d$ holes.[26] In Ag they can only be screened by a rather diffuse $5s$-type orbital, whereas in Pd we have partial $4d$ screening as indicated above. There is no appreciable modulation in Ag because the shake-off process takes place like in an atom with one hole in the intermediate state and two holes in the final state, practically unscreened. The reversed modulation in Pd with respect to ^1G illustrates the less atomic-like change of the corresponding potential. In Ru and Rh, there is a *fully* screened $3d^8$, screened by a $4d$-type orbital. The strong screening inhibits the shake process but as shown above results in a satellite. In conclusion, we have presented a consistent interpretation of the $L_{2,3}M_{4,5}M_{4,5}$ satellites in the $4d$ metals using accurate threshold measurements in combination with a single-step scattering approach.

The work of J.E.H. was sponsored by the Stichting Nationale Computerfaciliteiten (National Computing Facilities Foundation, NCF) for the use of supercomputer facilities with financial support from the Nederlandse Organisatie voor Wetenschappelijk Onderzoek (Netherlands Organization for Scientific Research, NWO). The work of T.Å. was supported by the Academy of Finland.

*Present address: MaxLab, Lund University, P.O. Box 118, S-22100 Lund, Sweden.

[1] H. Aksela *et al.*, Phys. Rev. Lett. **79**, 4970 (1997).
[2] E. Kukk *et al.*, Phys. Rev. Lett. **76**, 3100 (1996).
[3] O. Björneholm *et al.*, Phys. Rev. Lett. **79**, 3150 (1997).
[4] C. Keller *et al.*, Phys. Rev. Lett. **80**, 1774 (1998).
[5] C. O. Almbladh and L. Hedin, in *Handbook on Synchrotron Radiation*, edited by E. E. Koch (North-Holland, Amsterdam, 1983), Vol. 1.
[6] D. D. Sarma *et al.*, Phys. Rev. Lett. **63**, 656 (1989); **66**, 967 (1991).
[7] J. C. Fuggle and G. A. Sawatzky, Phys. Rev. Lett. **66**, 966 (1991).
[8] W. Drube, R. Treusch, and G. Materlik, Phys. Rev. Lett. **74**, 42 (1995).
[9] M. Weinelt *et al.*, Phys. Rev. Lett. **78**, 967 (1997).
[10] N. Mårtensson and B. Johansson, Phys. Rev. B **28**, 3733 (1983).
[11] D. D. Sarma *et al.*, Phys. Rev. B **40**, 12 542 (1989).
[12] S. R. Barman and D. D. Sarma, J. Phys.: Condens. Matter **4**, 7607 (1992).
[13] D. D. Sarma *et al.*, Phys. Rev. B **48**, 6822 (1993).
[14] D. D. Sarma and P. Mahadevan, Phys. Rev. Lett. **81**, 1658 (1998).
[15] M. Cini, Solid State Commun. **24**, 681 (1977).
[16] G. A. Sawatzky, Phys. Rev. Lett. **39**, 504 (1977).
[17] J.-M. Mariot and M. Ohno, Phys. Rev. B **34**, 2182 (1986).
[18] G. Kleiman, R. Landers, and S. G. C. de Castro, J. Electron Spectrosc. Relat. Phenom. **68**, 329 (1994).
[19] R. Landers, G. Kleiman, and S. G. C. de Castro, J. Electron Spectrosc. Relat. Phenom. **72**, 211 (1995).
[20] G. G. Kleiman *et al.*, Phys. Rev. B **58**, 16 103 (1998).
[21] R. D. Cowan, *The Theory of Atomic Structure and Spectra* (University of California Press, Berkeley, 1981).
[22] The L_3 binding energy ranges from 2838 eV (Ru) to 3551 eV (Ag). The corresponding L_2-L_3 splitting increases from 129 eV to 173 eV.
[23] W. Drube *et al.*, J. Electron Spectrosc. Relat. Phenom. **88-91**, 683 (1998).
[24] T. Åberg, Phys. Scr. **T41**, 71 (1992).
[25] T. Åberg and B. Crasemann, in *Resonant Anomalous X-ray Scattering*, edited by G. Materlik, C. J. Sparks, and K. Fischer (North-Holland, Amsterdam, 1994), p. 430.
[26] G. G. Kleiman *et al.*, Phys. Rev. B **44**, 3383 (1991).